Supporting Information

Diverse Configurations of Columnar Liquid Crystals in Cylindrical Nano- and Micropores

Rui-bin Zhang,[†,§] Goran Ungar,[†, §,*] Xianbing Zeng,[§] Zhihao Shen[‡]

[†] Department of Physics, Zhejiang Sci-Tech University, Xiasha College Park, Hangzhou 310018, China
[§] Department of Materials Science and Engineering, University of Sheffield, Sheffield S1 3JD, United Kingdom
[‡] Key Laboratory of Polymer Chemistry and Physics of Ministry of Education, Center for Soft Matter Science and Engineering, and College of Chemistry and Molecular Engineering, Peking University, Beijing 100871, China

Contents

S1. Calculation of correlation length of HAT6 in 35 and 60 nm pores

S1.1 Determination of the diffraction spot broadening

In order to correct for instrumental broadening the profile of the primary synchrotron beam in the focal, i.e. detector plane was determined. We used two different standards with highly ordered crystal structure, n-alkane $C_{40}H_{82}$ (99% pure, Sigma-Aldrich) and silver behenate (AgBe) (provided by the Diamond Light Source), both with powder-like diffraction patterns. Both compounds gave a series of reflection orders, and the peak widths of these reflections were extrapolated to $q = 0$ to correct for the effect of lattice strain in the reference samples. The peaks were fitted to a Gaussian profile, and the peak width Δq is the full width at half height of the Gaussian.

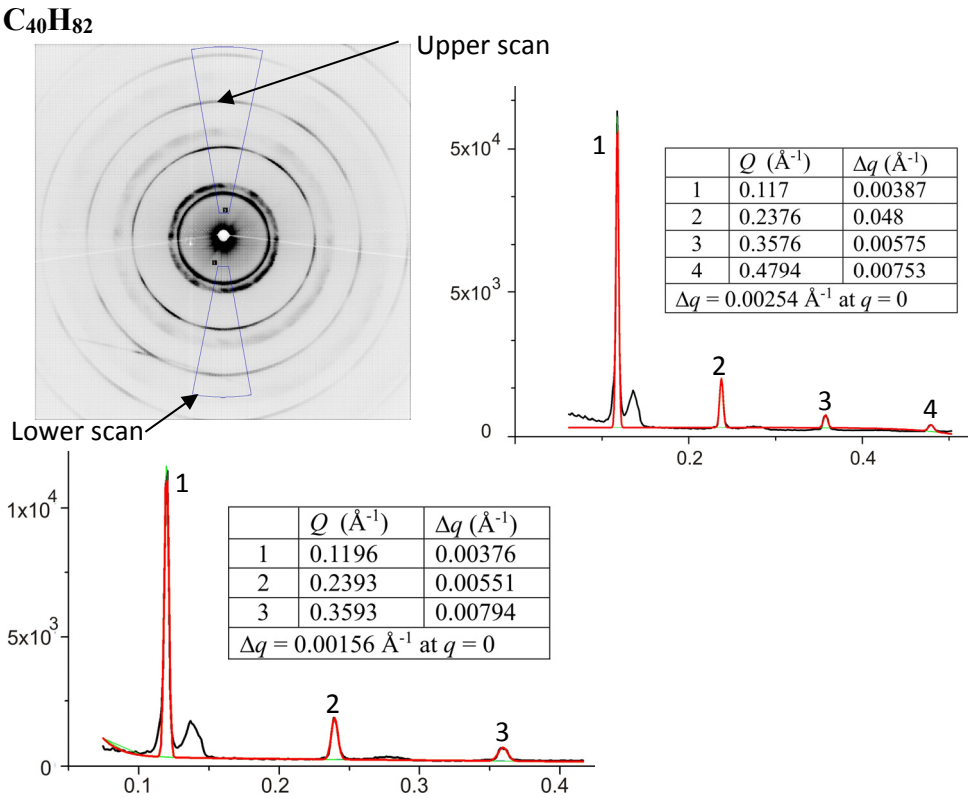

Figure S1. Determination of instrumental broadening using $C_{40}H_{82}$.

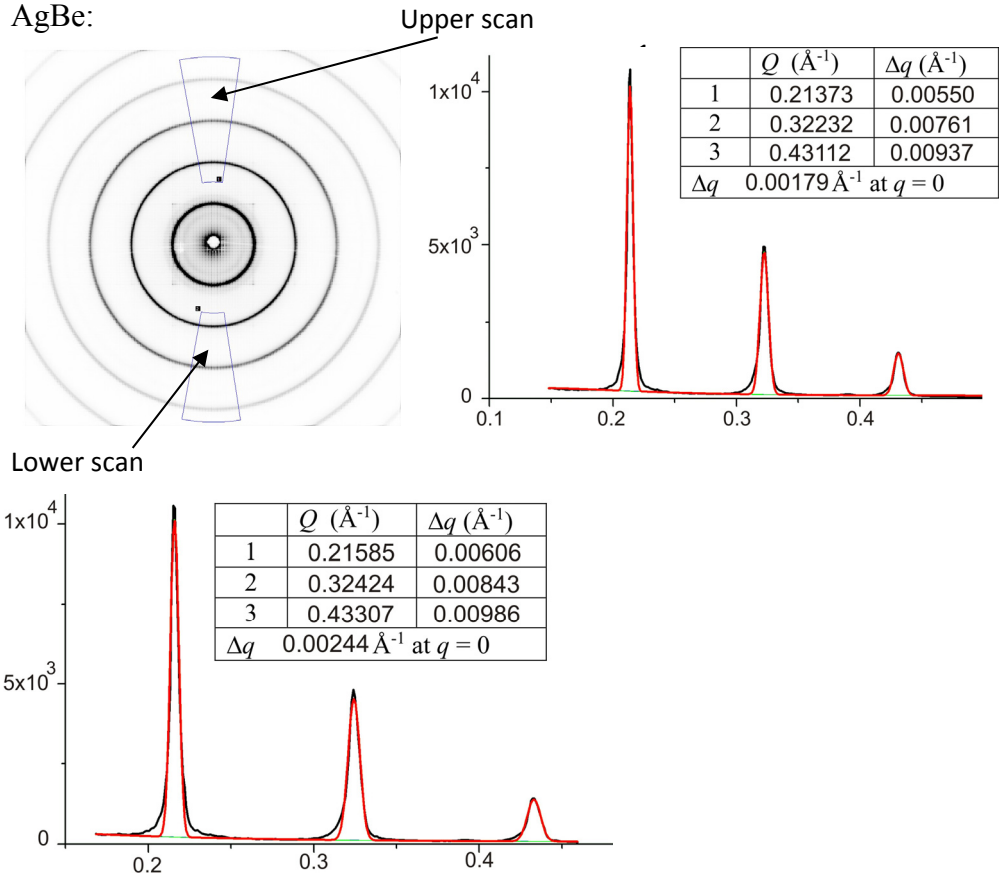

Figure S2. Determination of instrumental broadening using Ag Behenate.

Taking the average of the above four extrapolated Δq values gives an estimation of the peak width of the direct beam as Δq_0=0.0021 Å^{-1}.

S1.2. Determination of intrinsic line widths and coherence length

The instrumental peak width was subtracted from the Gaussian profile fitted to the experimental peak, taking advantage of the property that the sum of the widths of two Gaussian functions is equal to the width of their convolution. The coherence length ξ was calculated using the Scherrer equation.

.

S1.2.1. HAT6 in 35 nm AAO template

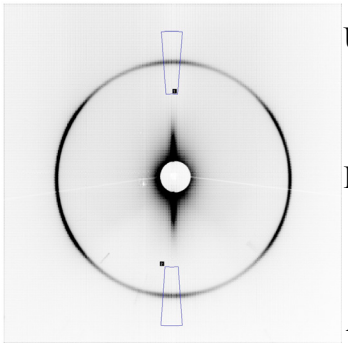

Upper scan: $\Delta q_1 = 0.02239$ Å^{-1}

$\xi_1 = 2\pi/(\Delta q_1 - \Delta q_0) = 309$ Å

Lower scan: $\Delta q_2 = 0.02213$ Å^{-1}

$\xi_2 = 2\pi/(\Delta q_2 - \Delta q_0) = 314$ Å

Average: $\xi = 312$ Å

Figure S3. Determination of coherence length ξ of **HAT6** in 35 nm AAO template.

S1.2.2. HAT6 in 60 nm AAO template

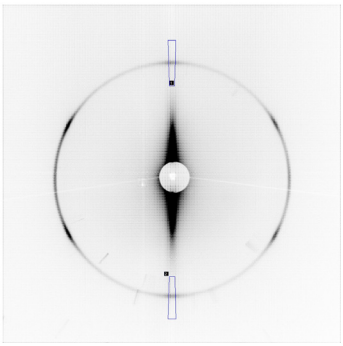

Upper scan: $\Delta q_1 = 0.01277$Å^{-1}

$\xi_1 = 2\pi/(\Delta q_1 - \Delta q_0) = 589$ Å

Lower scan: $\Delta q_2 = 0.01299$ Å^{-1}

$\xi_2 = 2\pi/(\Delta q_2 - \Delta q_0) = 577$ Å

Average: $\xi = 583$ Å

Figure S4. Measurement of the line width of the equatorial (100) reflection of **HAT6** in the 60 nm AAO template

S2. Wide-angle X-ray diffraction pattern showing axial orientation of HAT6 in a 100 µm ID glass capillary

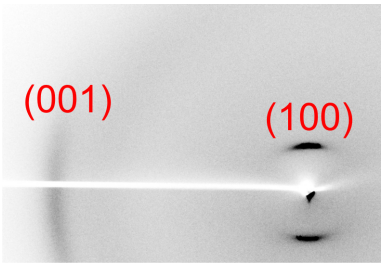

Figure S5. X-ray diffraction pattern of **HAT6** axially oriented in a 100 µm ID glass capillary. The (100) and (001) reflections correspond to the intercolumnar *d*-spacing of 16.2 Å and the intra-columnar disc-to-disc distance of 3.41 Å, respectively.

S3. SAXS patterns and corresponding models of Bola in a 50 µm ID glass capillary

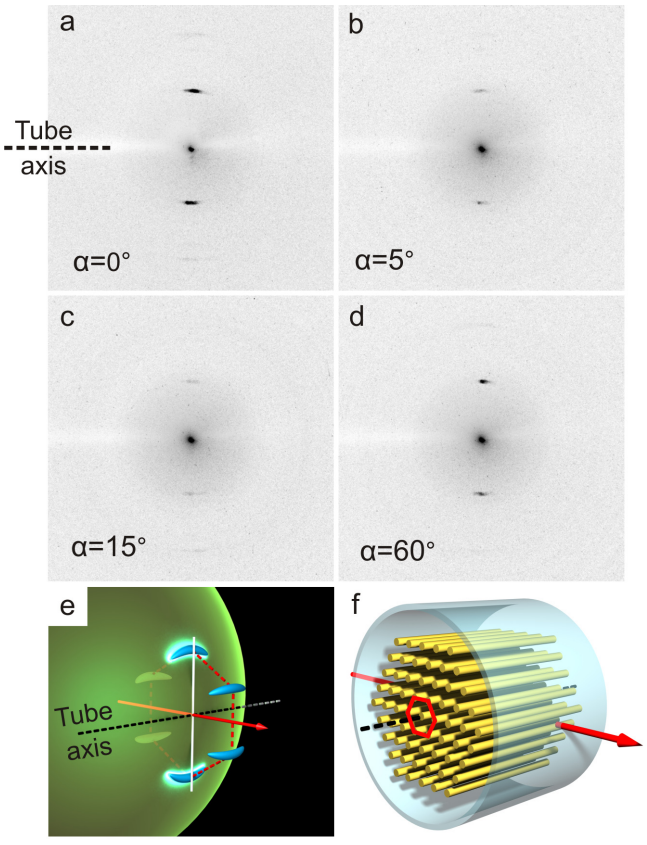

Figure S6. (a-d) SAXS patterns of **Bola** in a 50 µm ID glass capillary. The rotation angle α around the capillary tube is arbitrarily assigned to 0° when the strong {10} reflections show up on the equator (vertical direction). (e). corresponding reciprocal space cutting the Ewald sphere. (f). axially oriented **Bola** inside the capillary.